Highly Efficient Preparation of Multiscaled Quantum Dot Barcodes for Multiplexed Hepatitis B Detection

Gang Wang,[†] Yuankui Leng,[†] Hongjing Dou,[†,*] Lu Wang,[†] Wanwan Li,[†] Xiebing Wang,[†] Kang Sun,[†,*] Lisong Shen,[‡] Xiangliang Yuan,[‡] Jiyu Li,[‡] Kun Sun,[‡] Junsong Han,[§] Huasheng Xiao,[§] and Yue Li[§]

[†]The State Key Lab of Metal Matrix Composites, School of Materials Science and Engineering, Shanghai Jiao Tong University, Shanghai 200240, People's Republic of China, [‡]Xin Hua Hospital, School of Medicine, Shanghai Jiao Tong University, Shanghai 200092, People's Republic of China, and [§]Shanghai Biochip Co., Ltd. & National Engineering Center for Biochip at Shanghai, 151 Libing Road, Zhangjiang Hi-Tech Park, Pudong, Shanghai, 201203, People's Republic of China

ABSTRACT Both disease diagnosis and therapeutic treatments require real-time information from assays capable of identifying multiple targets. Among various multiplexed biochips, multiplexed suspension assays of quantum dot (QD)-encoded microspheres are highly advantageous. This arises from the excellent fluorescent properties of the QDs incorporated into these microspheres, thus allowing them to serve as "QD barcodes". QD barcodes can be prepared through various approaches. However, the formulation of improved synthetic techniques that may allow more efficient preparation of QD barcodes with better encoding accuracy still remains a challenge. In this report, we describe a combined membrane emulsification—solvent evaporation (MESE) approach for the efficient preparation of QD barcodes. By combining the advantages of the MESE approach in controlling the barcode sizes with accurate encoding, a three-dimensional barcode library that integrates the signals of the forward scattering, fluorescence 1, and fluorescence 4 channels was established *via* flow cytometry. The five indexes of hepatitis B viruses were chosen as diagnostic targets to examine the feasibility of the QD barcodes in high-throughput diagnosis. On the basis of showing that singleplex detection is feasible, we demonstrate the ability of these QD barcodes to simultaneously and selectively detect a multitude of diverse biomolecular targets.

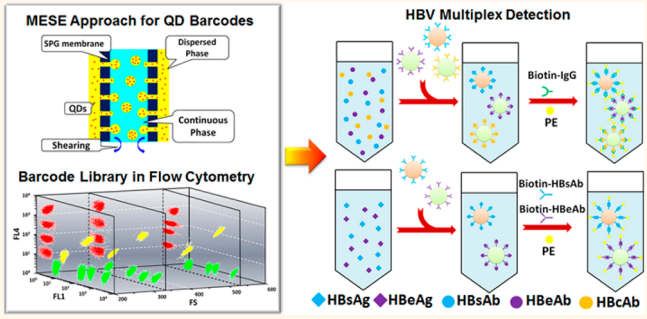

KEYWORDS: quantum dots · microspheres · Shirasu porous glass membrane emulsification · flow cytometry · suspension immunoassay

The development of both disease diagnosis and therapeutic treatment requires real-time information from multiple targets, such as genes and proteins, to establish a universal identification of biological entities. Multiplexed biochips, which facilitate parallel target recognition, provide the most promising way to achieve this goal. Among the two families of mainstream multiplexed arrays, which include planar arrays and suspension arrays, multiplexed suspension arrays of encoded microspheres offer various advantages. These advantages include fast binding kinetics, flexibility in target selection, and well-controlled binding conditions.[1,2] Consequently, these systems have received significant attention since the first commercial multiplexed suspension array was developed by Luminex Co.[3]

The barcoding of microspheres used in suspension arrays is the core technology supporting multiplexed suspension arrays. As demonstrated by the Luminex system, microspheres can be encoded with fluorescent organic dye molecules of various wavelengths and intensities to create a library of barcodes allowing parallel detection of multiple targets.[3] However, there are only a limited number of spectrally well-resolved organic dyes that do not interfere with commonly used biological markers,[1,4] which limits the number of available barcodes. Moreover, multiple excitation lasers are typically required if the dyes have different excitation wavelengths, which increases both the cost and the bulk of the decoding instrumentation. Various strategies involving barcodes have been proposed to overcome the limitations of organic dyes for coding.

* Address correspondence to hjdou@sjtu.edu.cn, ksun@sjtu.edu.cn.

Received for review September 29, 2012 and accepted December 3, 2012.

Published online December 03, 2012
10.1021/nn3045215

Spectroscopic (*e.g.*, quantum dot, upconversion nanocrystal, and Raman signature-based barcodes),[5−10] graphical,[11,12] magnetic,[13] physical (*e.g.*, physical characteristics including size and refractive index),[14,15] and molecular (*e.g.*, DNA)[16] signatures have all been explored. As natural substitutes for organic dyes to create barcodes, quantum dots (QDs) provide excellent and unique optical properties. These properties include narrow and symmetrical emission spectra, broad excitation wavelengths (*e.g.*, QDs with different emissions can be excited by a single wavelength excitation source), tunable emission wavelengths, and high brightness.[17] All of these advantages position QDs as ideal candidates for the creation of diverse barcodes for suspension assays. The spectroscopic encoding of microspheres based on the colors and intensities of QDs has been seen as the most promising approach, owing to its flexible barcoding and convenient decoding.[18,19]

Since their conception in 2001 by the Nie group,[5] QD barcodes have been prepared through various approaches.[5,20−32] According to the order of the microsphere synthesis and QD encoding steps, these approaches can be categorized as two strategies, including the "microsphere first" strategy and the "microsphere combined encoding" strategy. Two approaches have been developed for the microsphere first strategy, including the "swelling approach"[5,20−22] and "layer-by-layer (LBL) assembly",[23−25] which involved embedding QDs within the interiors of microspheres or depositing QDs onto the surfaces of microspheres, respectively. However, these two approaches usually result in surface-level loading of QDs onto the polymer.[5,22] Consequently, the QDs are exposed to the environment, which may destabilize their fluorescence intensities.[21] The fluorescent intensities of QD barcodes can be significantly improved by the "solvent evaporation approach" proposed by us.[26] However, the fluorescent stabilities of the QD barcodes fabricated through this strategy remain limited, and this procedure requires that the QDs be encapsulated deep within the polymer matrix. On the basis of this consideration, the microsphere combined encoding strategy was developed to allow the encapsulation of QDs within the interiors of the microsphere barcodes during the microsphere fabrication stage.[27−30] However, this strategy usually did not improve the fluorescence properties or the size distributions of the resultant microspheres. Recently, Chan *et al.* implemented the microsphere combined encoding strategy by using linear polystyrene (PS) in a concentration-controlled flow focusing (CCFF) technique to obtain narrowly dispersed QD-in-PSMA (where PSMA denotes poly(styrene-*co*-maleic anhydride)) microspheres.[31] This technique greatly promoted the applications of QD barcodes.[31,32] However, a limitation of this technique is that it requires a specialized continuous flow focusing apparatus, and microspheres smaller than 4 μm cannot yet be prepared. Moreover, the productivity (3×10^6 microspheres/mL per hour) of this technique is not high enough to meet the requirements of commercial mass production. The formulation of more efficient synthetic techniques needed to advance QD barcode production still remains a challenging task.

In the present work, we show that the problems noted above can be resolved by the development of a combined membrane emulsification−solvent evaporation (MESE) approach. Shirasu porous glass (SPG) membrane emulsification was chosen for this approach because it is very effective in improving the uniformity of emulsions, thus providing good size control for the emulsion droplet fabrication.[33−35] Consequently, the sizes of the resultant QD-encoded microspheres can be readily controlled by adjusting the membrane pore size.[36] By introducing the forward scattering (FS) signal of flow cytometry, which corresponds to the barcode size into the encoding of microsphere barcodes, we take full advantage of the MESE approach in flexibly controlling the barcode size. This allowed us to establish a three-dimensional barcode library that integrates the signals of the FS, fluorescence 1 (FL1), and fluorescence 4 (FL4) channels of flow cytometry. Furthermore, the five indexes of hepatitis B viruses (HBV) were chosen as diagnostic targets to examine the effectiveness of the QD barcodes for high-throughput diagnosis.

RESULTS AND DISCUSSION

As illustrated in Scheme 1, the MESE approach comprises two steps: (1) emulsification of the dispersed phase into the continuous phase by using a SPG membrane, and (2) a subsequent solvent evaporation step to obtain the solid QD barcodes. In the first step, the organic phase containing QDs and polymers serves as the dispersed phase and is pushed by nitrogen pressure through the SPG membrane pores into the emulsifier-containing aqueous phase. In comparison with the CCFF technique, this approach provides a significant efficiency improvement. Taking the barcode generation of using 1 μm pore SPG membrane as an example, the efficiency could be improved more than 1000-fold, with a droplet generation efficiency of $\sim 2 \times 10^{10}$ droplets/mL per hour. As shown by the optical microscopy images of the emulsion droplets obtained *via* SPG membrane emulsification in Figure S1 of the Supporting Information, there was no obvious difference between the QD-free emulsion droplets and the emulsion droplets that incorporated QDs. The laser confocal fluorescence (LCF) and scanning electron microscopy (SEM) images of the resultant 520 nm QD barcodes (obtained by encapsulating 520 nm CdSe/CdS/ZnS QDs) are shown in Figure S2 of the Supporting Information. The two-step MESE approach shown in Scheme 1 provided an effective method to generate robust barcodes with homogeneous QD encapsulation, smooth surfaces, and narrow size distributions. First, in comparison with other emulsification methods, SPG membrane emulsification

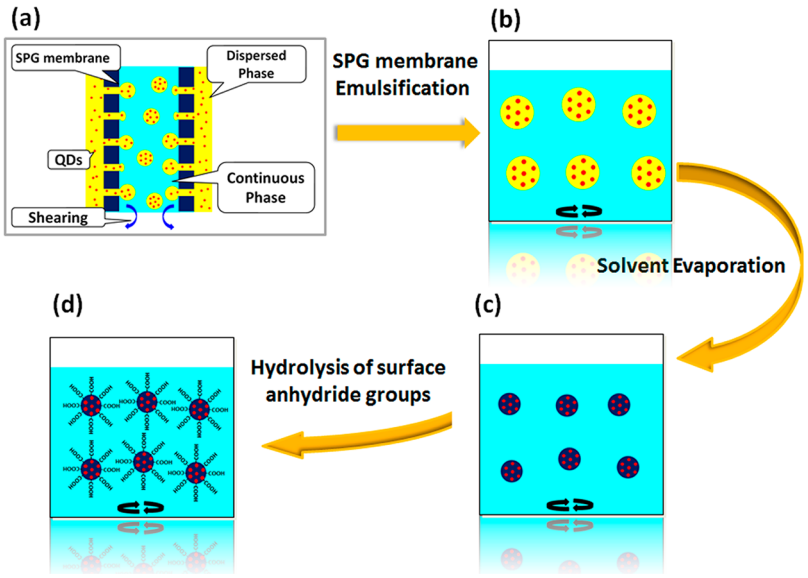

Scheme 1. Schematic illustration showing the preparation of QD barcodes with surface carboxyl groups by the MESE approach. These steps include (a) introduction of the QD-bearing dispersed phase droplets into the aqueous phase *via* passage through a SPG membrane to form QD-encapsulating emulsion droplets, (b) dispersal of the emulsion droplets into the aqueous phase *via* magnetic stirring during the emulsification process, (c) solvent evaporation treatment to form QD barcodes, (d) hydrolysis treatment to yield QD barcodes bearing carboxyl groups on their surfaces. In this approach, the compositions of the dispersion phase and the continuous phase are, respectively, a QD/polymer-containing organic phase and an emulsifier-containing aqueous phase.

proceeds under milder conditions. The low shear force employed during membrane emulsification helps to maintain the original fluorescence properties of the QDs and thus allows accurate encoding of the microspheres. Considering the complex situation involved in the fabrication of nanocrystal−polymer composite microspheres due to the interactions between the surface ligands of the nanocrystals and the polymer matrix,[37,38] the present study provides the first report on generating QD-encoded microspheres *via* SPG membrane emulsification. Subsequently, during the solvent evaporation step, PSMA polymers gradually become solidified from the surface to the interior as the solvent evaporates. The exterior-to-interior progression of this solidification process ensures the complete and homogeneous encapsulation of the QDs. Inspired by Chan's work,[31] PSMA was selected for this investigation as a model polymer to demonstrate the MESE approach, as this polymer serves both to protect the QDs and also to provide functional groups. The anhydride groups can easily be hydrolyzed to form carboxyl groups, which are frequently used to immobilize biomolecules.[39]

Considering the advantages of the MESE approach, we tried to combine a physical signature (*i.e.*, size) with spectroscopic encoding, to create a more diverse barcode library equipped with three variables in contrast with currently existing libraries that only utilize spectroscopic signatures.[5−8,31] As mentioned above, SPG membrane emulsification allows flexible control of emulsion droplet sizes. In this approach, a membrane with the appropriate pore size can be chosen according to the size desired for the droplets, which thus facilitates the size encoding of the barcodes. In addition, the mild conditions utilized for the MESE approach also facilitate the accurate encoding of microspheres by allowing one to adjust the concentration of the QD solution during the first step. Figure 1 demonstrates individual microscopy images and corresponding emission spectra of 12 QD barcodes, in which the microspheres were encoded by utilizing three size levels and four intensity levels. Through the combination of size and fluorescent signatures, we established a 12 barcode library by using only one kind of QD (520 nm CdSe/CdS/ZnS QDs). The size control of the barcode microspheres was accomplished by using three different membranes with the pore sizes of 1.0, 3.0, and 4.9 μm. Meanwhile, the fluorescence intensity signature was implemented by using QD solutions with various concentrations in the MESE approach. Theoretically, the number of barcodes would increase exponentially with the addition of more variables to the encoding process;[5] therefore, the content of the library can be expected to expand further by increasing the variable levels.

The size-tunable emission wavelength and narrow emission spectra facilitate the spectroscopic encoding of the QD barcodes. Here we synthesized CdSe/CdS/ZnS and CdTeSe/CdS/ZnS QDs with five distinct emission wavelengths ranging from 480 to 680 nm (see Figure S3 in the Supporting Information). By utilizing these five different color-emitting QDs, we realized one-color and two-color encoding of the QD barcodes. Figure 2a,b shows the individual images and corresponding emission spectra for each of the one-color and two-color QD barcodes. For two-color encoding, the relative intensities

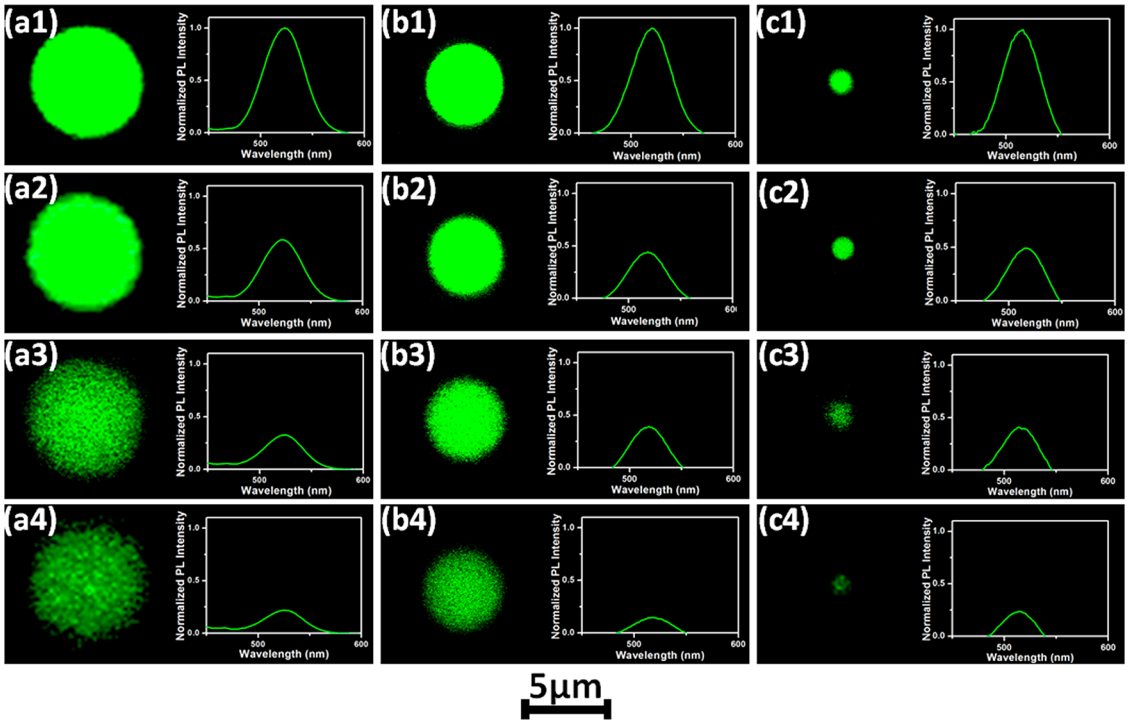

Figure 1. Individual microscopy images and corresponding emission spectra of 12 types of 520 nm QD barcodes, in which the microspheres were encoded by utilizing three size levels and four intensity levels. Images (a1−a4), (b1−b4), and (c1−c4) show the three families of barcodes prepared using 4.9, 3.0, and 1.0 μm pore diameters of SPG membranes, respectively.

of the two emission peaks were controlled by adjusting the relative ratios of the two kinds of QDs in the original QD-PSMA solution. As revealed by our study, the fluorescence spectra of the QD barcodes deviate slightly from that of the QD-PSMA solution (see Figure S4 in the Supporting Information). This deviation likely originates from the shrinkage of the barcodes during the solvent evaporation step. Taking the 520 nm barcode fabricated using the 4.9 μm membrane as an example, the diameters of the QD-PSMA droplets shrink from 16.7 to 6.6 μm for the resultant solid barcode during the solvent evaporation step, which corresponds to a 15-fold shrinkage of volume. Distance-dependent optical effects, such as Förster resonance energy transfer (FRET), will occur during this process. In addition, the photoluminescence of one QD overlapped with the absorption profile of another QD. The combination of these factors may have caused the changes observed in the final relative intensity levels of the individual QD emissions. However, despite this deviation, the validity of the MESE approach for accurately encoding QD barcodes can still be verified by the unique spectroscopic signatures displayed by each two-color barcode.

The most critical property of a QD barcode is its stability against changes to the external environments.[20,31] We therefore monitored the photoluminescence intensity of a 6.6 μm QD barcode encoded with 520 nm QDs against various temperatures (ranging from 4 to 80 °C) and a wide range of pH conditions (ranging from pH 1 to 13). The results demonstrated that the barcodes prepared by the MESE approach were stable against almost every perturbation that we introduced (see Figures S5 and S6 in the Supporting Information). This stability was achieved because the QDs are homogeneously dispersed throughout the polymer matrix rather than embedded close to the surface of the barcodes. After solving issues relating to the production efficiency, the encoding accuracy, and the stability of QD barcodes, we attempted to explore an appropriate approach to realize their applications in multiplexed detection.

As a versatile approach to detect both spectroscopic and size signatures, flow cytometry has been established as an effective technique for detecting multiplexed assays.[40] Although an expanded number of available QD barcodes is appealing, the specific detection requirements of a given instrument must be considered when evaluating the performance of a QD-barcode-based immunoassay. Actually, in a flow-cytometry-based immunoassay, a QD barcode library including numerous barcodes with distinct spectroscopic signatures may not be able to provide the same number of available barcodes in flow cytometric histograms.[40] There are two essential requirements for QD barcodes to be detectable *via* flow cytometry: (1) the emission of a barcode must be located within the detection channels of the flow cytometer, and (2) the code corresponding to each barcode should be distinguishable within the flow cytometric histograms. The fluorescence detection channels of the flow cytometer used in our study were 525 ± 15, 575 ± 15, 610 ± 15, 675 ± 15, and

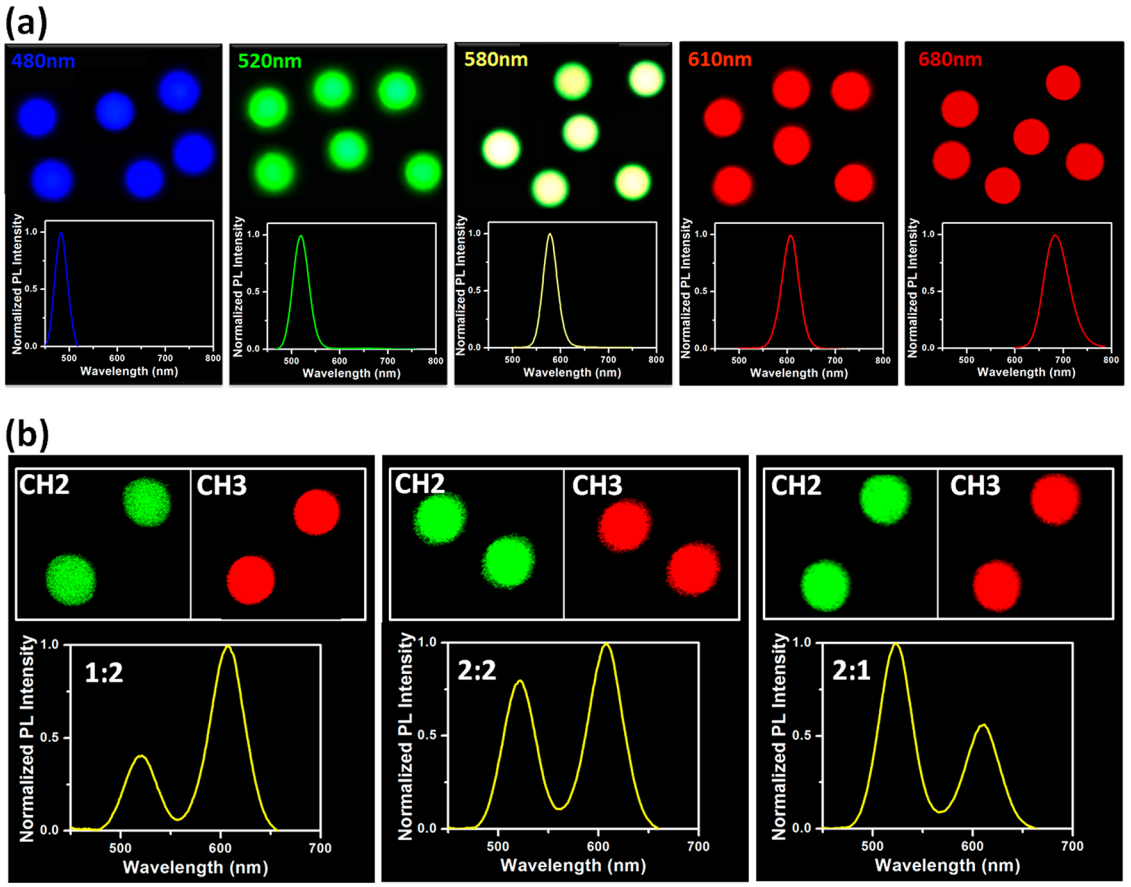

Figure 2. QD barcodes (6.6 μm) labeled with single- and dual-color encoding. Microscopy images and corresponding photoluminescence spectra of 6.6 μm QD barcodes containing (a) single-color encoding and (b) two-color encoding (the two emission wavelengths are 520 and 610 nm). Fluorescence microscopy images were recorded using a laser confocal microscope. Two detectors were utilized here, including channel 2, which was set for wavelengths ranging from 509 to 560 nm, and channel 3, which was set for wavelengths longer than 560 nm.

755 $\pm$ 15 nm (FL1 to FL5, respectively). Figure 3a is a diagram summarizing the five classes of one-color QD barcodes used in our study. As indicated by the figure, the 480 nm barcode was not detectable by the flow cytometer because it could not be excited by either of the two excitation light sources (488 and 633 nm). On the other hand, the 580 or 610 nm barcodes were also not suitable for preparing a flow-cytometry-based immunoassay because they could be detected simultaneously by two channels (FL2 and FL3). The comparison between barcode emissions and detection channels indicated that the 520 and 680 nm barcodes were both suitable for preparing a flow-cytometry-based barcode library. It should be noted that, by using QD barcodes, we only required a single 488 nm laser to excite all of the QD barcodes due to their broad excitation wavelengths. This feature would be very helpful for decreasing the amount of equipment required and thus reducing testing costs.

By combining the size signature (which is correlated to the signal intensity of the FS channel) together with the fluorescence signatures, a three-dimensional barcode library combining the signals in the FS, FL1, and FL4 channels can be established *via* flow cytometry. On the basis of this idea, a triple-parameter dot-plot was obtained (as shown in Figure 3b), in which each dot represents the signal from one type of QD barcode detected by the flow cytometer. As illustrated in Figure 3c, we have designed a shorthand nomenclature when referring to these barcodes that takes into account the wavelengths, relative intensities, as well as the sizes of the barcodes. This shorthand nomenclature consists of a letter and four digits, in which the letters A, B, and C denote the three barcodes fabricated by 1.0, 3.0, and 4.9 μm SPG membranes, respectively. Meanwhile, a four-digit number uses the hundreds digits of the wavelengths and the relative intensity. The first and third digits of this number are used to represent the wavelength, while the second and fourth numbers represent the intensity. For example, the number 5161 refers to a barcode containing 520 and 680 nm QDs at relative intensity levels of 1 and 1, respectively. By using two colors at four intensity ratios, combined with three size levels, we generated 30 individual QD barcodes with distinct signals, which are displayed in Figure 3c. Therefore, code A(B or C)5160 to 5460 corresponds to 520 nm QD barcodes with fluorescence intensities ranging from the lowest to the highest levels,

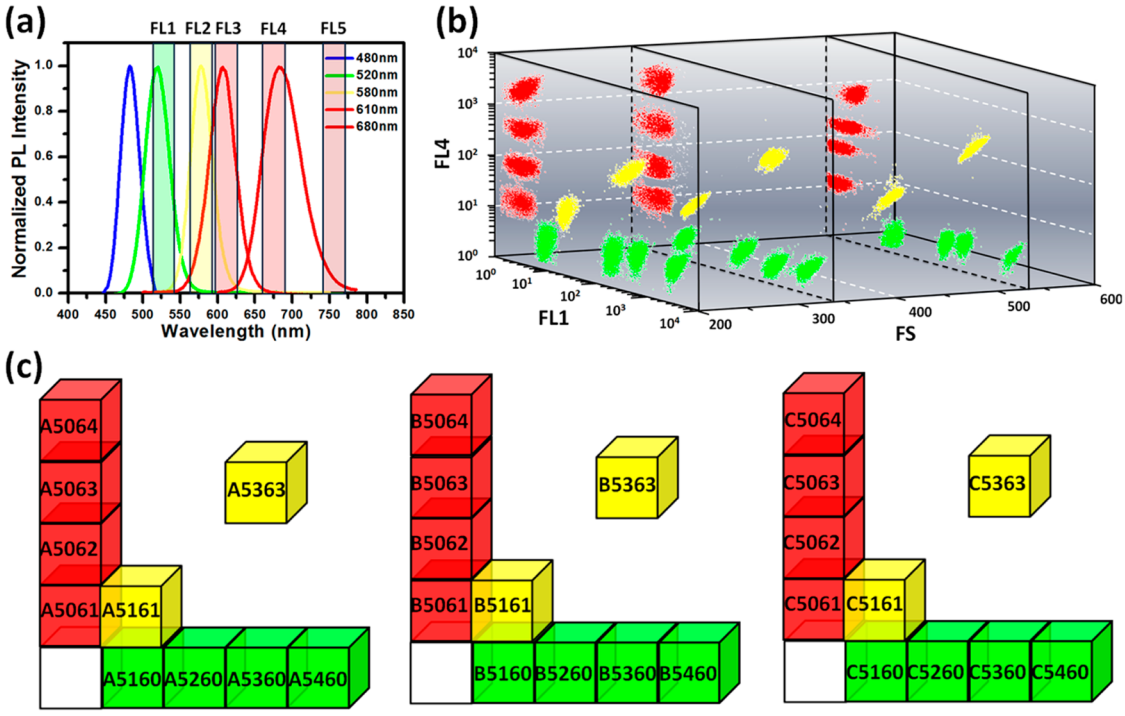

Figure 3. Relationship between fluorescence spectra of five single-color QD barcodes and the five detection channels of the flow cytometer (a). Barcode library showing three-dimensional dot map plots obtained *via* flow cytometry (b). Schematic illustration of the shorthand nomenclature (c).

respectively. Meanwhile, code A(B or C)5061 to 5064 correspond to 680 nm QD barcodes with fluorescence intensities ranging from the lowest to highest levels, respectively.

Available barcodes promised the feasibility of suspension multiplex assays. In the present work, we selected antibodies and antigens of hepatitis B viruses (HBV) as diagnostic targets. The reason for choosing these targets is the demand for high-throughput diagnosis of five indexes of HBV. The use of microsphere barcodes is an ideal tool to fulfill this demand.[41] HBV is a major health concern and cause of mortality worldwide. Approximately 2 billion people have been infected with HBV, and about 350 million live with chronic infection.[42] To confirm the phase of HBV infection, the concentration of HBV antigens/antibodies in the serum of patients is a credible immune index for general HBV diagnosis.[43,44] Five indexes, including hepatitis B surface antigens (HBsAg), hepatitis B e antigens (HBeAg), hepatitis B surface antibodies (HBsAb), hepatitis B e antibodies (HBeAb), and hepatitis B core antibodies (HBcAb), were analyzed in this study. Therefore, for our suspension immunoassays, three codes were selected for these five indexes. Code C5064 was assigned for HBsAg/HBsAb assays, code C5360 was assigned for HBcAb assays, and code C5260 corresponded to HBeAg/HBeAb assays. As shown in Scheme 2, the QD barcodes were conjugated with capture antigens or antibodies (denoted as CAs), which can conjugate to a target antibody or antigen (denoted as TA). This TA can also conjugate onto an anti-antibody (IgG) or an antibody that is conjugated with the dye phycoerythrin (PE). The size and optical signature of the barcode identifies the TA since different CAs are coated onto different emitting QD barcodes. A library of QD barcodes conjugated with CAs was placed into a vial along with the secondary anti-antibody/antibody-PE conjugates (denoted as SAPE). When a TA was introduced into the vial, that TA recognized both the QD barcodes and the SAPE, thereby assembling the QD barcode and SAPE together (Scheme S1 in the Supporting Information illustrates the sandwich structures of these HBV immunoassays). By measuring the optical emission of this assembled complex in a flow cytometer, a positive detection is observed when a fluorescence signal arises from both the QDs inside the barcodes and from PE at the same time. For flow cytometry analysis, 10 000 QD barcodes with sandwich immunoassay structures were excited by a 488 nm laser. The species of the captured target molecules were determined and classified according to the codes of the QD barcodes. In addition, the concentrations of the target molecules in the samples were closely related to the median fluorescence intensities (MFI) of the labeled PE reporters. The MFI of the PE reporters were detected in the FL2 channel and calculated from the data collected from 10 000 QD barcodes. Qualitative and quantitative analysis of the samples was therefore achieved. The recipes of all buffers used in the suspension immunoassays and the protocols for preparing and detecting the immunoassays are described in the Supporting Information.

Our experiments showed that the concentration of the CAs significantly affected the MFI values exhibited

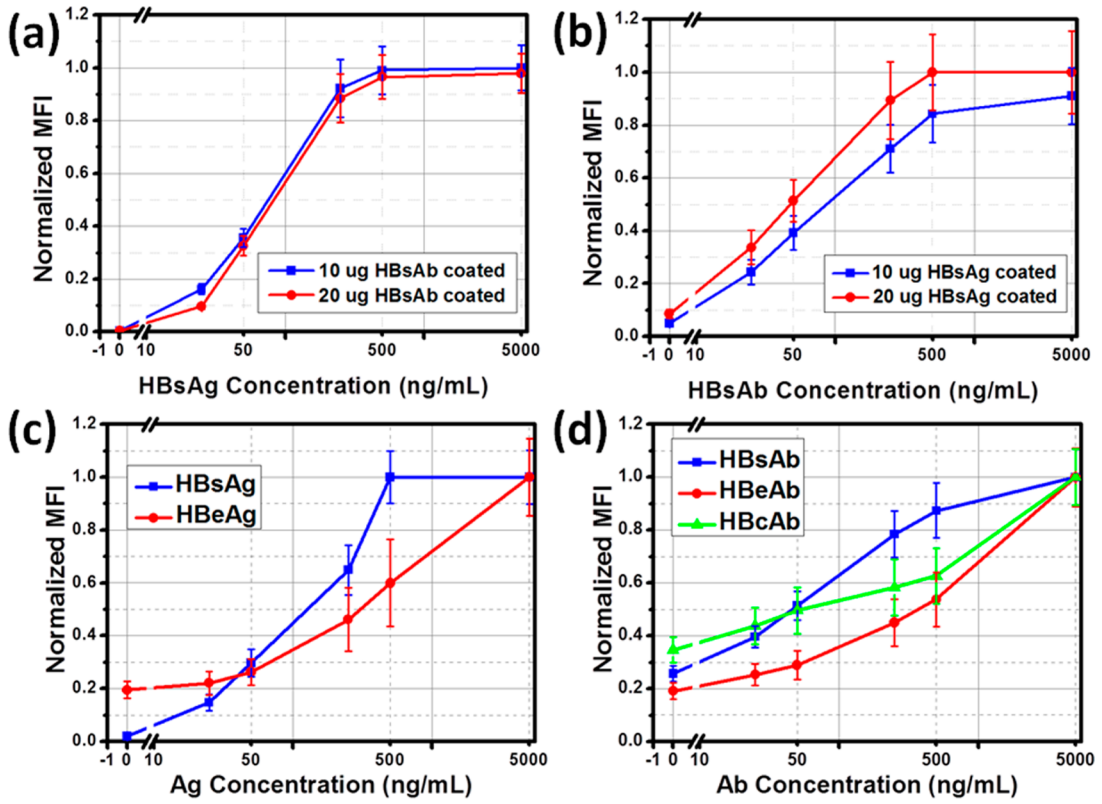

Figure 4. (a,b) Sensitivity plots of singleplex immunoassays for HBsAg and HBsAb detection. To optimize the CA concentrations, 10 and 20 μg of CAs was used per 1.25 $\times$ 10^5 microspheres, and the results are respectively compared. (c,d) Sensitivity plots of multiplex immunoassays for antigen and antibody detection, respectively. For HBsAg, HBeAg, and HBcAb immunoassays, 10 μg of CAs was used per 1.25 $\times$ 10^5 beads, whereas for HBsAb and HBeAb immunoassays, 20 μg of CAs was used per 1.25 $\times$ 10^5 beads. The amount of the coating antigens/antibodies was optimized to ensure the better detection sensitivity.

by the PE reporters for the resultant sandwich structures. As shown in Figure 4a, the MFI was slightly higher when we added 10 μg of HBsAb CAs per 1.25 $\times$ 10^5 microspheres for conjugation to the TAs compared with the MFI observed when we added 20 μg of CAs. This indicates that 10 μg of HBsAb CAs was sufficient for HBsAg detection, while excess CAs could inhibit the conjugation to a TA due to steric effects.[45] Meanwhile, for HBsAb detection, 20 μg of HBsAg CAs per 1.25 $\times$ 10^5 microspheres provided better MFI values than observed when only 10 μg was used (Figure 4b). Similar experiments for HBeAg, HBeAb, and HBcAb detection demonstrated that appropriate concentrations of corresponding CAs were 10, 20, and 10 μg per 1.25 $\times$ 10^5 microspheres, respectively (as shown in the Figure S7 in the Supporting Information). In all subsequent studies, we used these optimal CA concentrations for each assay since the multiplexing capabilities of the QD barcodes were not affected at this optimal range of 10 to 20 μg of CAs per 1.25 $\times$ 10^5 barcodes. The only factor to be affected was the analytical sensitivity.

The ability to detect multiple biomarkers in the same sample is crucial for high-throughput diagnosis. While we have already shown that singleplex detection is feasible, successful multiplex detection using multiple barcodes in a single vial would significantly speed up the diagnostic process. Before conducting multiplex detection tests, we purposely incubated a specific TA with various QD barcodes coated with different CAs to determine if cross-reactivity can occur. Our experiments show that the QD barcodes are able to distinguish the matching TAs against those that do not match. The ability of the QD barcodes to select and measure the different nontargeted antigens/antibodies was validated by conducting tests involving different combinations, the results are shown in Figures S8–S12 of the Supporting Information. Finally, we demonstrated that three barcodes could be used to detect two antigens or three antibodies in the same vial. The procedure for multiplex detection is illustrated in Scheme 2c. Buffer solutions were incubated with either both of the antigen-conjugated QD barcodes or all three of the antibody-conjugated QD barcodes. As shown in Figure 4c, after spiking both of the target antigens and SAPE for an incubation period of 10 min, we were able to detect both of these antigens simultaneously. Similarly, all three antibodies can also be detected simultaneously by spiking the three target antibodies and SAPE for an incubation period. These results conclusively demonstrate the ability of these QD barcodes to selectively detect a multitude of different target antigens or antibodies simultaneously in the

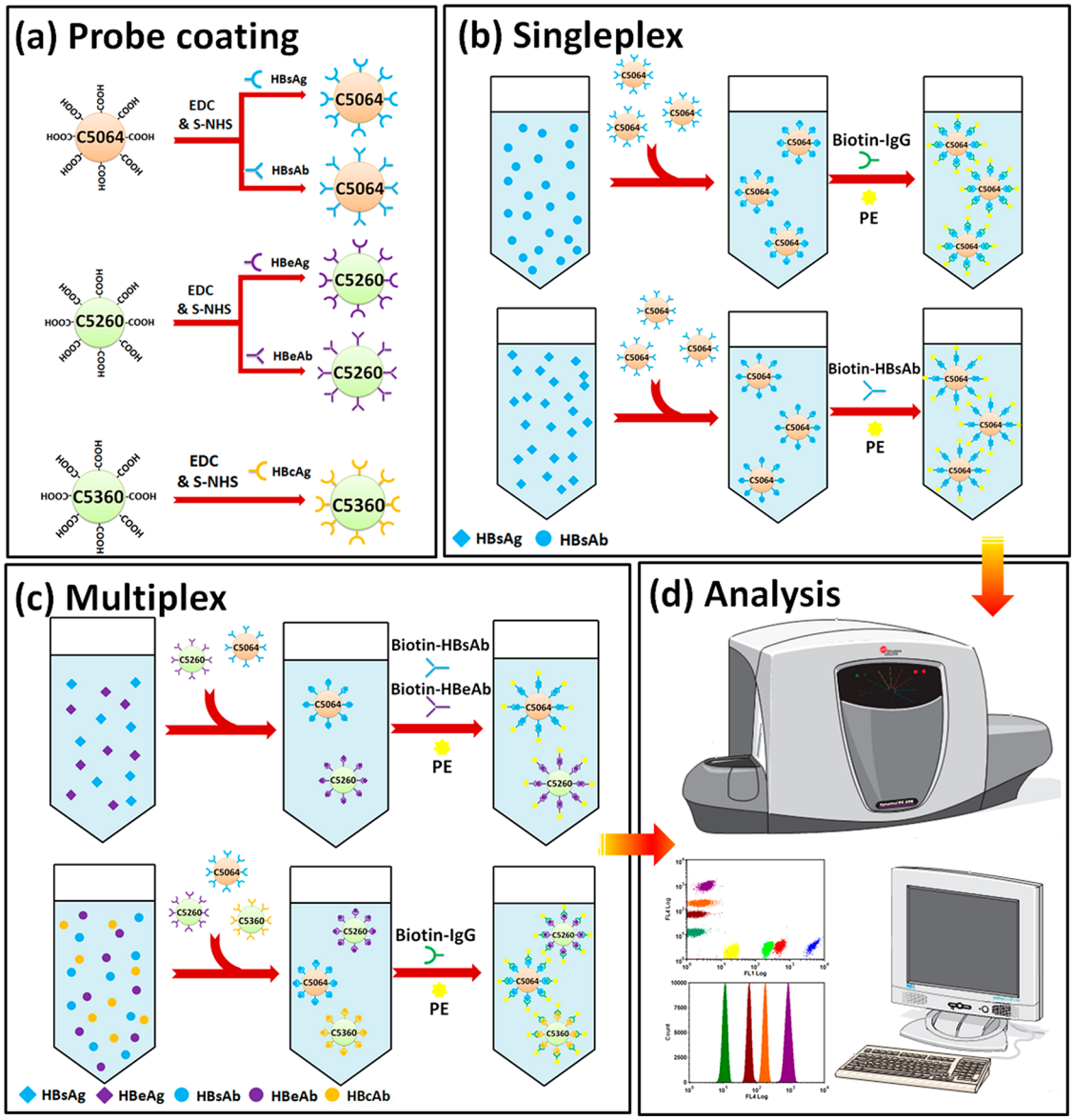

Scheme 2. Schematic diagram of the QD barcode assays, showing their interactions with the corresponding antigens and antibodies (a). Flowchart showing the sequential steps involved in singleplexed detection in the assay (b). Flowchart showing the sequential steps involved in multiplexed detection in the assay (c). Schematic diagram of the flow cytommetry system and outputs from analysis of the assays (d).

same buffer solution. In order to confirm the effectiveness of the QD barcodes in detecting HBV indexes of patient serum, we compared the HBsAg concentration of three serum samples (getting from one strong positive patient, one weakly positive patient, and one negative patient) detected by commercial HBV serum marker diagnostic assay and QD barcode-based assay, and results are shown in Figure S13. The results indicated that, although the commercial HBV assay was more sensitive, the concentration difference between the negative and positive samples obtained from QD barcode assays is more obvious compared with that obtained from commercial HBV assay. The detection concentrations from these two methods are comparable.

CONCLUSION

In conclusion, we have developed a membrane emulsification combined solvent evaporation (MESE) approach to fabricate QD-encoded microsphere barcodes with controllable sizes and accurate encoding. By the combination of encoding barcode sizes and their fluorescence signatures together, a three-dimensional barcode library which combines the signals of the FS, FL1, and FL4 was established using flow cytometry. We believe that the introduction of the FS signal to barcode encoding will provide many advantages for the MESE approach and enrich QD barcode libraries. Moreover, we demonstrated the capability of QD barcodes to rapidly detect and distinguish between five HBV indexes in a single sample.

Our results suggest that the QD barcodes generated by the MESE approach can provide feasible platforms for both singleplex and multiplex HBV detection.

METHODS

Fabrication of QD Barcodes by the MESE Approach. The CdSe/CdS/ZnS QDs were synthesized as described in the literature.[46] To prepare the CdTeSe/CdS/ZnS QDs, the core CdTeSe QDs were first synthesized according to a previously reported procedure,[47] in which the initial molar ratio of Cd to the total amount of Se and Te in the reaction solution was kept constant at 2:1 (Cd/Se + Te). Subsequently, the S precursor (S powder dissolved in TOP) was injected dropwise into the core QD solution to form the CdS shell. The Zn precursor (zinc stearate dissolved in paraffin) was then injected dropwise into the solution, and the temperature of the solution was kept at 200 °C to grow the ZnS shell. The solution was subsequently cooled to 80 °C and maintained at this temperature for 30 min. Finally, the solution was cooled to room temperature. The CdSe/CdS/ZnS and CdTeSe/CdS/ZnS QDs were purified by repeated (≥2) cycles in which the QDs were precipitated from solution with methanol and chloroform, centrifuged, and finally redispersed into toluene for further use.

To fabricate QD barcodes, a SPG membrane emulsification device (MG-20, SPG membrane/SPG Technology Co., Ltd.) was employed. First, two phases of an O/W emulsion were prepared individually. To prepare the dispersed oil phase, a designated amount of hydrophobic QDs and 0.5 g of PSMA were dissolved into 8 mL of toluene. The continuous aqueous phase was prepared by dissolving the anionic stabilizer SDS into 200 mL of deionized water at a concentration of 0.5 wt %. A hydrophilic SPG membrane with a specific pore size was then placed in the SPG membrane emulsification device. The oil phase and aqueous phase were stored in corresponding tanks within the device. Subsequently, the oil phase permeated through the membrane pores into the continuous aqueous phase under an optimized nitrogen pressure (for the barcode fabrication of using 1.0, 3.0, and 4.9 μm membranes, the optimized pressures are 15, 7, and 5 kPa, respectively). O/W emulsion droplets then formed on the surface of the membrane and were stabilized by the SDS surfactant. The continuous phase was gently magnetically stirred, so that the stabilized oil droplets were sheared away from the surface of the membrane and suspended into the aqueous phase. After all of the oil dispersion phase was sheared from the membrane, the emulsification generation was stopped by reducing the nitrogen pressure. Meanwhile, the aqueous solution was continuously stirred to help accelerate the evaporation of toluene from the emulsion droplets at room temperature. This stirring was continued for 24 h to ensure that all of the toluene had been evaporated. The final suspension was washed with deionized water and then ethanol and subsequently collected *via* centrifugation after each wash. The surfaces of the QD barcodes were modified to generate carboxyl groups following procedures described in the Supporting Information. Finally, the QD barcodes were freeze-dried to allow storage for further use.

Fluorescence Properties of QD Barcodes. Fluorescence spectra of the QD barcodes (1.5×10^7 barcodes/mL in water) were recorded using a Shimadzu RF-5301PC spectrofluorophotometer. Fluorescence images of the QD barcodes were recorded at various focalized planes in water using a laser scanning confocal microscope (LSM 510 META, Zeiss). True-color fluorescence images of the QD barcodes in water were recorded using a fluorescence microscope (IX-71, Olympus) equipped with a 100 W mercury arc lamp as the excitation source.

Flow Cytometric Analysis. A flow cytometer (FC500, Beckman Coulter) was used to analyze the suspension immunoassays and establish the barcode library. QD barcodes suspended in aqueous solutions were injected into the flow cytometer and were excited by a 488 nm laser. Signals from 10 000 microspheres were collected for each sample.

CA Conjugation onto the Surfaces of the QD Barcodes. Five different buffer solutions were used for the conjugation of CAs onto the surfaces of the QD barcodes. These buffers included a phosphate buffer saline (PBS) buffer, a washing buffer, an active buffer, a blocking buffer, and a storage buffer. The recipes for preparing the five buffers are listed in Table S1 of the Supporting Information. A 100 μL aqueous suspension of QD barcodes (1.25×10^6/mL) was washed three times with the washing buffer. Each sample was centrifuged and resuspended into 100 μL of the active buffer. A 10 μL solution of sulfo-NHS (50 mg/mL in active buffer) and 10 μL of 1-ethyl-3-(3-dimethylaminopropyl)carbodiimide hydrochloride (EDC) solution (50 mg/mL in active buffer) were then added to the sample. After incubation for 20 min on a vortex mixer at room temperature, the sample was washed three times with washing buffer, subsequently centrifuged, and then resuspended into 500 μL of PBS buffer. A designated quantity of CAs was subsequently added into the sample and incubated for 12 h on a vortex mixer at 10 °C. Thereafter, the sample was washed three times with the washing buffer and was then resuspended in 150 μL of blocking buffer for another 20 min to block the free carboxylates on the surface of the QD barcodes. Finally, the blocked CAs conjugated onto the QD barcodes were washed with washing buffer and stored in a storage buffer at 4 °C.

HBV Suspension Immunoassays. In addition to the washing buffer, a detection buffer and an assay buffer were used for the suspension immunoassays, and their recipes are also listed in Table S1 of the Supporting Information. Three different tests were conducted to study the sensitivity and cross-reactivity of the QD barcodes in HBV suspension immunoassays. The procedures of these tests were as follows:

Singleplex Detection. A 100 μL TA sample with a designated TA concentration (ranging from 0 to 5000 ng/mL in PBS buffer) was added into a single well of a 96-well plate with ultrafiltration membranes at the bottom. Subsequently, 2×10^4 CA-conjugated QD barcodes were added into the sample. After the sample was incubated for 1 h on a vortex mixer at room temperature, the sample was washed with washing buffer *via* filtration to remove the uncaptured TAs. Then 100 μL of SA solution (50 μg/mL biotin-conjugated secondary anti-antibodies or 10 μg/mL biotin-conjugated secondary antibodies in assay buffer) was added to the sample. The sample was then vortexed for 1 h at room temperature and then washed with washing buffer *via* filtration to remove the unreacted SAs. Subsequently, 100 μL of PE solution (1 μg/mL in the detection buffer) was added to the sample. After the sample was vortexed for 10 min at room temperature, it was washed with washing buffer *via* filtration to remove the unreacted PE. Finally, the QD barcodes in the sample were resuspended into 100 μL of the assay buffer for subsequent flow cytometric analysis.

Multiplex Detection. Various QD barcodes that were conjugated with a specific CA were added simultaneously into an assay containing various corresponding TA species that were mixed together. Each species of TA had a concentration ranging between 0 and 5000 ng/mL. A similar procedure as that employed for singleplex was then followed, in which the amount of SA and PE were regulated as the increasing number of TA species.

Cross-Reaction Study. QD barcodes conjugated with nonspecific CAs were added to TA samples, where nonspecific CAs refer to CAs that do not match the TA in the sample. A similar procedure was followed as that followed for singleplex detection.

Conflict of Interest: The authors declare no competing financial interest.

Acknowledgment. We acknowledge the National Natural Science Foundation of China (Nos. 20904032, 21174082, 50902093), the Science and Technology Committee of Shanghai (Project No. 10520706500), SMC-Chen Xing Young Scholars Awards of Shanghai Jiao Tong University, Open Fund of the State Key Lab of Metal Matrix Composites, and the Scientific Research Foundation for Returned Overseas Chinese Scholars from the State Education Ministry for funding this project. We thank the Instrumental Analysis Center of Shanghai Jiao Tong

University for assistance with the measurements. We also thank Shanghai Sunny New Technology Development Co., Ltd. for their support.

Supporting Information Available: TEM images of the QDs, as well as SEM and LSM images of the QD barcodes are provided. In addition, fluorescence stability analysis data on the QD barcodes, detailed surface modification procedures for the QD barcodes, preparation protocols for the buffers, a schematic illustration of sandwich suspension immunoassays for HBV detection, and other results determined from the suspension immunoassays of HBV are also provided. This material is available free of charge *via* the Internet at http://pubs.acs.org.

Note Added after ASAP Publication: After this paper was published online December 12, 2012, corrections were made to the Supporting Information. The corrected Supporting Information was reposted January 7, 2013.

REFERENCES AND NOTES

1. Wilson, R.; Cossins, A. R.; Spiller, D. G. Encoded Microcarriers for High-Throughput Multiplexed Detection. *Angew. Chem., Int. Ed.* **2006**, *45*, 6104–6117.
2. Finkel, N. H.; Lou, X.; Wang, C.; He, L. Barcoding the Microworld. *Anal. Chem.* **2004**, *76*, 352A–359A.
3. Fulton, R. J.; McDade, R. L.; Smith, P. L.; Kienker, L. J.; Kettman, J. R. Advanced Multiplexed Analysis with the Flowmetrix(Tm) System. *Clin. Chem.* **1997**, *43*, 1749–1756.
4. Sukhanova, A.; Nabiev, I. Fluorescent Nanocrystal-Encoded Microbeads for Multiplexed Cancer Imaging and Diagnosis. *Crit. Rev. Oncol. Hematol.* **2008**, *68*, 39–59.
5. Han, M.; Gao, X.; Su, J. Z.; Nie, S. Quantum-Dot-Tagged Microbeads for Multiplexed Optical Coding of Biomolecules. *Nat. Biotechnol.* **2001**, *19*, 631–635.
6. Dejneka, M. J.; Streltsov, A.; Pal, S.; Frutos, A. G.; Powell, C. L.; Yost, K.; Yuen, P. K.; Muller, U.; Lahiri, J. Rare Earth-Doped Glass Microbarcodes. *Proc. Natl. Acad. Sci. U.S.A.* **2003**, *100*, 389–393.
7. Lutz, B. R.; Dentinger, C. E.; Nguyen, L. N.; Sun, L.; Zhang, J.; Allen, A. N.; Chan, S.; Knudsen, B. S. Spectral Analysis of Multiplex Raman Probe Signatures. *ACS Nano* **2008**, *2*, 2306–2314.
8. Zhang, F.; Shi, Q.; Zhang, Y.; Shi, Y.; Ding, K.; Zhao, D.; Stucky, G. D. Fluorescence Upconversion Microbarcodes for Multiplexed Biological Detection: Nucleic Acid Encoding. *Adv. Mater.* **2011**, *23*, 3775–3779.
9. Pelaz, B.; Jaber, S.; de Aberasturi, D. J.; Wulf, V.; Aida, T.; de la Fuente, J. M.; Feldmann, J.; Gaub, H. E.; Josephson, L.; Kagan, C. R.; *et al.* The State of Nanoparticle-Based Nanoscience and Biotechnology: Progress, Promises, and Challenges. *ACS Nano* **2012**, *6*, 8468–8483.
10. Delehanty, J. B.; Bradburne, C. E.; Susumu, K.; Boeneman, K.; Mei, B. C.; Farrell, D.; Blanco-Canosa, J. B.; Dawson, P. E.; Mattoussi, H.; Medintz, I. L. Spatiotemporal Multicolor Labeling of Individual Cells Using Peptide-Functionalized Quantum Dots and Mixed Delivery Techniques. *J. Am. Chem. Soc.* **2011**, *133*, 10482–10489.
11. Nicewarner-Pena, S. R.; Freeman, R. G.; Reiss, B. D.; He, L.; Pena, D. J.; Walton, I. D.; Cromer, R.; Keating, C. D.; Natan, M. J. Submicrometer Metallic Barcodes. *Science* **2001**, *294*, 137–141.
12. Fenniri, H.; Chun, S.; Ding, L.; Zyrianov, Y.; Hallenga, K. Preparation, Physical Properties, On-Bead Binding Assay and Spectroscopic Reliability of 25 Barcoded Polystyrene–Poly(ethylene glycol) Graft Copolymers. *J. Am. Chem. Soc.* **2003**, *125*, 10546–10560.
13. Kuramitz, H. Magnetic Microbead-Based Electrochemical Immunoassays. *Anal. Bioanal. Chem.* **2009**, *394*, 61–69.
14. Benecky, M. J.; Post, D. R.; Schmitt, S. M.; Kochar, M. S. Detection of Hepatitis B Surface Antigen in Whole Blood by Coupled Particle Light Scattering (Copalis(Tm)). *Clin. Chem.* **1997**, *43*, 1764–1770.
15. Lawrie, G. A.; Battersby, B. J.; Trau, M. Synthesis of Optically Complex Core–Shell Colloidal Suspensions: Pathways to Multiplexed Biological Screening. *Adv. Funct. Mater.* **2003**, *13*, 887–896.
16. Nam, J. M.; Stoeva, S. I.; Mirkin, C. A. Bio-Bar-Code-Based DNA Detection with PCR-like Sensitivity. *J. Am. Chem. Soc.* **2004**, *126*, 5932–5933.
17. Gill, R.; Zayats, M.; Willner, I. Semiconductor Quantum Dots for Bioanalysis. *Angew. Chem., Int. Ed.* **2008**, *47*, 7602–7625.
18. Chattopadhyay, P. K.; Price, D. A.; Harper, T. F.; Betts, M. R.; Yu, J.; Gostick, E.; Perfetto, S. P.; Goepfert, P.; Koup, R. A.; De Rosa, S. C.; *et al.* Quantum Dot Semiconductor Nanocrystals for Immunophenotyping by Polychromatic Flow Cytometry. *Nat. Med.* **2006**, *12*, 972–977.
19. del Mercato, L. L.; Abbasi, A. Z.; Ochs, M.; Parak, W. J. Multiplexed Sensing of Ions with Barcoded Polyelectrolyte Capsules. *ACS Nano* **2011**, *5*, 9668–9674.
20. Gao, X.; Nie, S. Doping Mesoporous Materials with Multicolor Quantum Dots. *J. Phys. Chem. B* **2003**, *107*, 11575–11578.
21. Lee, J. A.; Hung, A.; Mardyani, S.; Rhee, A.; Klostranec, J.; Mu, Y.; Li, D.; Chan, W. C. W. Toward the Accurate Read-out of Quantum Dot Barcodes: Design of Deconvolution Algorithms and Assessment of Fluorescence Signals in Buffer. *Adv. Mater.* **2007**, *19*, 3113–3118.
22. Bradley, M.; Bruno, N.; Vincent, B. Distribution of Cdse Quantum Dots within Swollen Polystyrene Microgel Particles Using Confocal Microscopy. *Langmuir* **2005**, *21*, 2750–2753.
23. Allen, C. N.; Lequeux, N.; Chassenieux, C.; Tessier, G.; Dubertret, B. Optical Analysis of Beads Encoded with Quantum Dots Coated with a Cationic Polymer. *Adv. Mater.* **2007**, *19*, 4420–4425.
24. Petukhova, A.; Paton, A. S.; Wei, Z.; Gourevich, I.; Nair, S. V.; Ruda, H. E.; Shik, A.; Kumacheva, E. Polymer Multilayer Microspheres Loaded with Semiconductor Quantum Dots. *Adv. Funct. Mater.* **2008**, *18*, 1961–1968.
25. Rauf, S.; Glidle, A.; Cooper, J. M. Application of Quantum Dot Barcodes Prepared Using Biological Self-Assembly to Multiplexed Immunoassays. *Chem. Commun.* **2010**, *46*, 2814–2816.
26. Wang, G.; Zhang, P.; Dou, H.; Li, W.; Sun, K.; He, X.; Han, J.; Xiao, H.; Li, Y. Efficient Incorporation of Quantum Dots into Porous Microspheres through a Solvent-Evaporation Approach. *Langmuir* **2012**, *28*, 6141–6150.
27. Lansalot, M.; Joumaa, N.; Theretz, A.; Elaissari, A. Synthesis of Quantum Dot-Tagged Submicrometer Polystyrene Particles by Miniemulsion Polymerization. *Langmuir* **2006**, *22*, 1810–1816.
28. O'Brien, P.; Cummins, S. S.; Darcy, D.; Dearden, A.; Masala, O.; Pickett, N. L.; Ryley, S.; Sutherland, A. J. Quantum Dot-Labelled Polymer Beads by Suspension Polymerisation. *Chem. Commun.* **2003**, 2532–2533.
29. Yang, Y.; Wen, Z.; Dong, Y.; Gao, M. Incorporating Cdte Nanocrystals into Polystyrene Microspheres: Towards Robust Fluorescent Beads. *Small* **2006**, *2*, 898–901.
30. Vaidya, S. V.; Gilchrist, M. L.; Maldarelli, C.; Couzis, A. Spectral Bar Coding of Polystyrene Microbeads Using Multicolored Quantum Dots. *Anal. Chem.* **2007**, *79*, 8520–8530.
31. Fournier-Bidoz, S.; Jennings, T. L.; Klostranec, J. M.; Fung, W.; Rhee, A.; Li, D.; Chan, W. C. W. Facile and Rapid One-Step Mass Preparation of Quantum-Dot Barcodes. *Angew. Chem., Int. Ed.* **2008**, *47*, 5577–5581.
32. Giri, S.; Sykes, E. A.; Jennings, T. L.; Chan, W. C. W. Rapid Screening of Genetic Biomarkers of Infectious Agents Using Quantum Dot Barcodes. *ACS Nano* **2011**, *5*, 1580–1587.
33. Mine, Y.; Shimizu, M.; Nakashima, T. Preparation and Stabilization of Simple and Multiple Emulsions Using a Microporous Glass Membrane. *Colloids Surf., B* **1996**, *6*, 261–268.
34. Omi, S.; Ma, G.; Nagai, M. Membrane Emulsification—A Versatile Tool for the Synthesis of Polymeric Microspheres. *Macromol. Symp.* **2000**, *151*, 319–330.
35. Ito, F.; Honnami, H.; Kawakami, H.; Kanamura, K.; Makino, K. Preparation and Properties of PLGA Microspheres Containing Hydrophilic Drugs by the SPG (Shirasu Porous Glass) Membrane Emulsification Technique. *Colloids Surf., B* **2008**, *67*, 20–25.
36. Vladisavljević, G. T.; Surh, J.; McClements, J. D. Effect of Emulsifier Type on Droplet Disruption in Repeated Shirasu Porous Glass Membrane Homogenization. *Langmuir* **2006**, *22*, 4526–4533.

37. Omi, S.; Kanetaka, A.; Shimamori, Y.; Supsakulchai, A.; Nagai, M.; Ma, G.-H. Magnetite (Fe_3O_4) Microcapsules Prepared Using a Glass Membrane and Solvent Removal. *J. Microencapsul.* **2001**, *18*, 749–765.
38. Takeda, M.; Tanabe, E.; Iwaki, T.; Yabuki, A.; Okuyama, K. Importance of Dispersibility of TiO_2 in Preparation of TiO_2-Dispersed Microspheres by Shirasu Porous Glass (SPG) Membrane Emulsification. *Adv. Powder Technol.* **2009**, *20*, 361–365.
39. Taitt, C. R.; Shriver-Lake, L. C.; Anderson, G. P.; Ligler, F. S. Surface Modification and Biomolecule Immobilization on Polymer Spheres for Biosensing Applications. *J. Biomed. Nanotechnol.* **2011**, *726*, 77–94.
40. Gao, X.; Nie, S. Quantum Dot-Encoded Mesoporous Beads with High Brightness and Uniformity-Rapid Readout Using Flow Cytometry. *Anal. Chem.* **2004**, *76*, 2406–2410.
41. Krishhan, V. V.; Khan, I. H.; Luciw, P. A. Multiplexed Microbead Immunoassays by Flow Cytometry for Molecular Profiling: Basic Concepts and Proteomics Applications. *Crit. Rev. Biotechnol.* **2009**, *29*, 29–43.
42. Tan, A. T.; Koh, S.; Goh, V.; Bertoletti, A. Understanding the Immunopathogenesis of Chronic Hepatitis B Virus: An Asian Prospective. *J. Gastroenterol. Hepatol.* **2008**, *23*, 833–843.
43. Wursthorn, K.; Mederacke, I.; Manns, M. P. Chronic Hepatitis B Pathophysiology, Diagnosis and Treatment Options. *Front. Gastrointest. Res.* **2010**, *26*, 32–41.
44. Aspinall, E. J.; Hawkins, G.; Fraser, A.; Hutchinson, S. J.; Goldberg, D. Hepatitis B Prevention, Diagnosis, Treatment and Care: A Review. *Occup. Med.* **2011**, *61*, 531–540.
45. Jennings, T. L.; Rahman, K. S.; Fournier-Bidoz, S.; Chan, W. C. W. Effects of Microbead Surface Chemistry on DNA Loading and Hybridization Efficiency. *Anal. Chem.* **2008**, *80*, 2849–2856.
46. Wang, X.; Li, W.; Sun, K. Stable Efficient CdSe/CdS/ZnS Core/Multi-Shell Nanophosphors Fabricated through a Phosphine-Free Route for White Light-Emitting-Diodes with High Color Rendering Properties. *J. Mater. Chem.* **2011**, *21*, 8558–8565.
47. Xing, B.; Li, W.; Wang, X.; Dou, H.; Wang, L.; Sun, K.; He, X.; Han, J.; Xiao, H.; Miao, J.; *et al.* Highly-Fluorescent Alloyed Quantum Dots of $CdSe_{1-x}Te_x$ Synthesized in Paraffin Liquid: Gradient Structure and Promising Bio-application. *J. Mater. Chem.* **2010**, *20*, 5664–5674.